

Suppression of Self-Induced Flavor Conversion in the Supernova Accretion Phase

Srdjan Sarikas,^{1,2} Georg G. Raffelt,² Lorenz Hüdepohl,³ and Hans-Thomas Janka³

¹*Dipartimento di Scienze Fisiche, Università di Napoli Federico II, 80126 Napoli, Italy*

²*Max-Planck-Institut für Physik (Werner-Heisenberg-Institut), Föhringer Ring 6, 80805 München, Germany*

³*Max-Planck-Institut für Astrophysik, Karl-Schwarzschild-Str. 1, 85748 Garching, Germany*

(Dated: 15 September 2011)

Self-induced flavor conversions of supernova (SN) neutrinos can strongly modify the flavor dependent fluxes. We perform a linearized flavor stability analysis with accretion-phase matter profiles of a $15 M_{\odot}$ spherically symmetric model and corresponding neutrino fluxes. We use realistic energy and angle distributions, the latter deviating strongly from quasi-isotropic emission, thus accounting for both multi-angle and multi-energy effects. For our matter and neutrino density profile we always find stable conditions: flavor conversions are limited to the usual Mikheyev-Smirnov-Wolfenstein effect. In this case one may distinguish the neutrino mass hierarchy in a SN neutrino signal if the mixing angle θ_{13} is as large as suggested by recent experiments.

PACS numbers: 97.60.Bw, 14.60.Pq

Introduction.—The huge neutrino fluxes emitted by core-collapse supernovae (SNe) are key to the explosion dynamics and nucleosynthesis [1] and detecting a high-statistics “neutrino light curve” from the next nearby SN is a major goal for neutrino astronomy [2]. Besides probing the core-collapse phenomenon in unprecedented detail, one may detect signatures of flavor oscillations and extract information on neutrino mixing parameters [3, 4].

The refractive effect caused by matter [5] suppresses flavor oscillations until neutrinos pass through the Mikheyev-Smirnov-Wolfenstein (MSW) region in the collapsing star’s envelope [6, 7]. However, neutrino-neutrino interactions, through a flavor off-diagonal refractive index [8, 9], can trigger self-induced flavor conversions [10–12]. This collective effect usually occurs between the neutrino sphere and the MSW region and can strongly modify neutrino spectra [13–15], although this would never seem to help explode the star [16]. Actually, in low-mass SNe (not studied here) the density falls off so fast that MSW can occur first, leading to novel effects on the prompt ν_e burst [17].

Collective oscillations at first seemed unaffected by matter because its influence does not depend on neutrino energies [13]. However, depending on emission angle, neutrinos accrue different matter-induced flavor-dependent phases until they reach a given radius. This “multi-angle matter effect” can suppress self-induced flavor conversion [18]. Based on schematic flux spectra, this was numerically confirmed for accretion-phase SN models where the density near the core is large [19]. This epoch, before the delayed explosion finally takes off, is when the neutrino luminosity and the difference between the $\bar{\nu}_e$ and $\bar{\nu}_{\mu,\tau}$ fluxes are largest. If self-induced flavor conversion did not occur and the mixing angle θ_{13} was not very small [20], the accretion phase would provide a plausible opportunity to determine the mass hierarchy [3, 19].

Numerical multi-angle simulations of collective oscillations are very demanding [21], but it is much easier to

study if such oscillations are suppressed for given density profile and neutrino distributions. Self-induced conversion requires that part of the spectrum is prepared in one flavor, the rest in another. The collective mode consists of pendulum-like flavor exchange between these parts without changing the overall flavor content [10, 22]. The inevitable starting point is a flavor instability of the neutrino distribution caused by neutrino-neutrino refraction. An exponentially growing mode can be detected with a linearized analysis of the evolution equations [12, 23]. We here apply this method to a numerical accretion-phase SN model, for the first time using both realistic neutrino energy spectra and angular distributions.

Numerical SN model.—Our spherically symmetric simulation of an accretion-phase SN model was performed with the PROMETHEUS-VERTEX code as in Ref. [24], now with a $15 M_{\odot}$ progenitor [25]. The transport module computes the energy and angle distributions of ν and $\bar{\nu}$ for all flavors by a tangent-ray discretization of the Boltzmann transport equation [26]. We used 21 nearly geometrically spaced energy bins up to 380 MeV and 672 tangent rays. We do not artificially trigger an explosion, but otherwise our model is comparable to Ref. [19]. We use several snapshots and illustrate our findings with one at 280 ms post bounce. The flux spectra (Fig. 1) show a ν_e excess from deleptonization and a $\bar{\nu}_e$ flux almost twice that of ν_x (representing any of $\nu_{\mu,\tau}$ or $\bar{\nu}_{\mu,\tau}$) and average ν_e , $\bar{\nu}_e$ and ν_x energies of 15.3, 18.1, and 16.9 MeV.

We study neutrino propagation in the free-streaming limit, so we can describe the angular distribution by the angle ϑ_R relative to the radial direction at a chosen inner-boundary radius R . Actually it is more convenient to use $u = \sin^2 \vartheta_R = (1 - \cos^2 \vartheta_r) r^2 / R^2$, which is uniformly distributed on $0 \leq u \leq 1$ if emission is isotropic at a “neutrino sphere” with radius R [18, 23]. We choose $R = 44.7$ km and show the corresponding u distribution in Fig. 1. Isotropic emission from a neutrino sphere is not a good description because neutrinos emerge from a

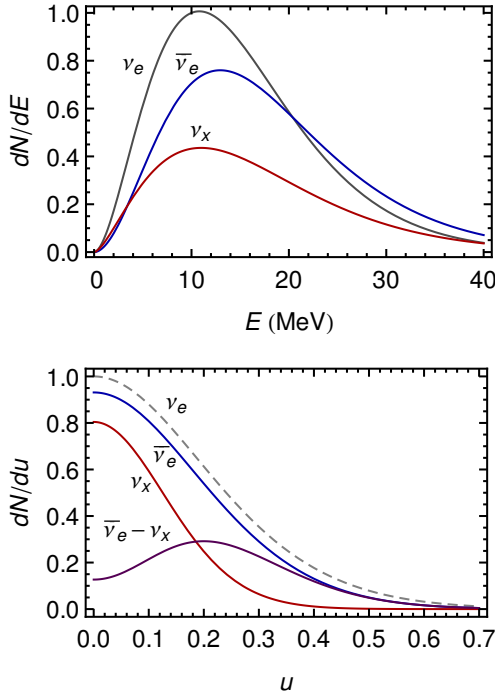


FIG. 1: Flux spectra for our 280 ms SN model. The angle variable $0 \leq u \leq 1$ is based on $R = 44.7$ km.

thick layer. The $\bar{\nu}_e$ and ν_x intensities are similar in the radial direction: the excess $\bar{\nu}_e$ flux largely arises from its broader angular distribution (larger emission region). Flavor oscillations depend on the difference of the e and x distributions, which is small in the radial direction (Fig. 1). The angular distributions do not cross, although in principle there could have been a forward ν_x excess.

In the context of neutrino oscillations, $\omega = \Delta m^2/2E$ is a preferred energy variable, where $\Delta m^2 = (50 \text{ meV})^2$ is the “atmospheric” neutrino mass-squared difference relevant for 1–3 oscillations studied here. Moreover, treating anti-neutrinos formally as negative-energy neutrinos with negative occupation numbers vastly simplifies the formalism. Flavor oscillations can exchange ν_e with ν_x , leaving the overall neutrino flux unchanged, so only $F_{\nu_e} - F_{\nu_x}$ matters. Our sign convention means that for anti-neutrinos we then use $F_{\bar{\nu}_x} - F_{\bar{\nu}_e}$, corresponding to the flavor isospin convention [13]. The neutrino flux difference distribution $g(\omega, u)$ thus defined is shown in Fig. 2. It is negative for anti-neutrinos ($\omega < 0$) because $F_{\bar{\nu}_e} > F_{\bar{\nu}_x}$. For $\omega \sim 0.2 \text{ km}^{-1}$ there is a spectral crossing as a function of u , i.e. for large E the ν_x flux does exceed the ν_e flux in the forward direction.

Self-induced oscillations exchange the positive and negative parts of $g(\omega, u)$, leaving fixed the overall flavor content $\varepsilon = (F_{\nu_e} - F_{\nu_x}) / (F_{\bar{\nu}_e} - F_{\bar{\nu}_x}) - 1 = \int d\omega du g(\omega, u)$. Our $g(\omega, u)$ is mostly negative for $\bar{\nu}$ and mostly positive for ν , so collective oscillations largely correspond to pair conversions $\nu_e \bar{\nu}_e \leftrightarrow \nu_x \bar{\nu}_x$. Accretion-phase distributions are “single crossed” in this sense, i.e. $g(\omega, u)$ changes sign

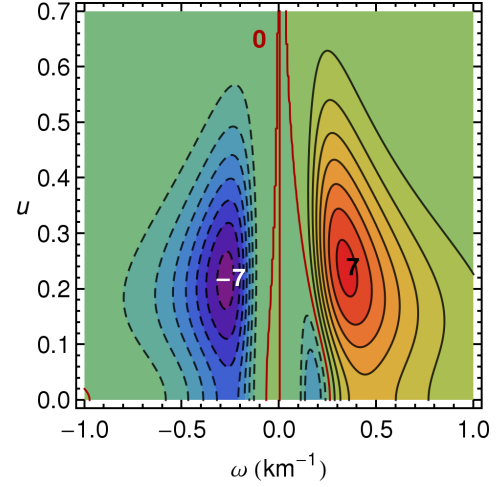


FIG. 2: Distribution $g(\omega, u)$ describing the neutrino fluxes.

essentially only on the line $\omega = 0$, because of the large excess of the ν_e and $\bar{\nu}_e$ fluxes. Significant multiple crossings are typical for the cooling phase [14].

Equations of motion (EoM).—We describe three-flavor neutrino propagation by energy- and angle-dependent 3×3 matrices $\Phi_{E,u}(r)$. Boldface characters denote matrices in flavor space. The diagonal $\Phi_{E,u}$ elements are the ordinary number fluxes $F_{E,u}^\alpha$ (flavor α) integrated over a sphere of radius r , with negative E and negative number fluxes for anti-neutrinos. The off-diagonal elements, which are initially zero, represent phase information caused by flavor oscillations. The flavor evolution is then provided by the “Schrödinger equation” $i\partial_r \Phi_{E,u} = [\mathbf{H}_{E,u}, \Phi_{E,u}]$ with the Hamiltonian [18]

$$\mathbf{H}_{E,u} = \frac{1}{v_u} \left(\frac{\mathbf{M}^2}{2E} + \sqrt{2} G_F \mathbf{N}_\ell \right) + \frac{\sqrt{2} G_F}{4\pi r^2} \int_{-\infty}^{+\infty} dE' \int_0^1 du' \frac{1 - v_u v_{u'}}{v_u v_{u'}} \Phi_{E',u'} . \quad (1)$$

The matrix \mathbf{M}^2 of neutrino mass-squares causes vacuum flavor oscillations and that of net charged lepton densities $\mathbf{N}_\ell = \text{diag}(n_e - n_{\bar{e}}, n_\mu - n_{\bar{\mu}}, n_\tau - n_{\bar{\tau}})$ adds the Wolfenstein matter effect. The third term provides neutrino-neutrino refraction and is analogous to matter except for Pantaleone’s off-diagonal elements and except that in the SN context neutrinos are not isotropic. A neutrino radial velocity at radius r is $v_u = (1 - u R^2/r^2)^{1/2}$. The factor $1 - v_u v_{u'}$ arises from the current-current nature of the weak interaction and causes multi-angle effects. Moreover, v_u appears in the denominator because we follow the flavor evolution projected on the radial direction, causing the multi-angle matter effect [18].

Up to the MSW region, the matter effect is so large that $\Phi_{E,u}$ is very nearly diagonal in the weak-interaction basis, the usual approximation made in SN neutrino transport. Neutrinos remain stuck in flavor eigenstates

unless the off-diagonal $\Phi_{E,u}$ elements start growing by the self-induced instability. To find the latter we linearize the EoM in the small off-diagonal amplitudes.

Stability condition.—We study the instability driven by the atmospheric Δm^2 and the mixing angle $\theta_{13} \ll 1$, we work in the two-flavor limit, and switch to the $\omega = \Delta m^2/2E$ variable. We write the flux matrices in the form

$$\Phi_{\omega,u} = \frac{\text{Tr } \Phi_{\omega,u}}{2} + \frac{F_{\omega,u}^e - F_{\omega,u}^x}{2} \begin{pmatrix} s_{\omega,u} & S_{\omega,u} \\ S_{\omega,u}^* & -s_{\omega,u} \end{pmatrix}, \quad (2)$$

where $F_{\omega,u}^{e,x}$ are the flavor fluxes at the inner boundary radius R . The flux summed over all flavors, $\text{Tr } \Phi_{\omega,u}$, is conserved in our free-streaming limit. The ν_e survival probability is $\frac{1}{2}[1 + s_{\omega,u}(r)]$ in terms of the “swap factor” $-1 \leq s_{\omega,u}(r) \leq 1$. The off-diagonal element $S_{\omega,u}$ is complex and $s_{\omega,u}^2 + |S_{\omega,u}|^2 = 1$.

The small-amplitude limit means $|S_{\omega,u}| \ll 1$ and to linear order $s_{\omega,u} = 1$. Assuming in addition a large distance from the source so that $1 - v_u \ll 1$, the evolution equation linearized in $S_{\omega,u}$ and in u is [23]

$$i\partial_r S_{\omega,u} = [\omega + u(\lambda + \varepsilon\mu)] S_{\omega,u} - \mu \int du' dw' (u + u') g_{\omega'u'} S_{\omega',u'}. \quad (3)$$

Weak-interaction effects are encoded in the r -dependent parameters with dimension energy

$$\begin{aligned} \lambda &= \sqrt{2} G_F [n_e(r) - n_{\bar{e}}(r)] \frac{R^2}{2r^2}, \\ \mu &= \frac{\sqrt{2} G_F [F_{\bar{\nu}_e}(R) - F_{\bar{\nu}_x}(R)]}{4\pi r^2} \frac{R^2}{2r^2}. \end{aligned} \quad (4)$$

The factor $R^2/2r^2$ signifies that only the multi-angle impact of the ν - ν and matter effects are relevant for the stability analysis, not the densities themselves. Both λ and μ depend on R , but so does the occupied u -range: physical results do not depend on the choice of R . We choose $R = 44.7$ km such that the occupied u -range is 0–1. We normalize the ν - ν interaction strength μ to the $\bar{\nu}_e$ - $\bar{\nu}_x$ flux difference at R , i.e. $\int_{-\infty}^0 d\omega \int_0^1 du g_{\omega,u} = -1$, but the only physically relevant quantity is $\mu(r) g_{\omega,u}$. Our SN model provides $\mu(R) = 1.73 \times 10^4 \text{ km}^{-1}$ and an “asymmetry” $\varepsilon = \int d\omega du g_{\omega,u} = 0.35$.

Writing solutions of the linear differential equation, Eq. (3), in the form $S_{\omega,u} = Q_{\omega,u} e^{-i\Omega r}$ with complex frequency $\Omega = \gamma + i\kappa$ and eigenvector $Q_{\omega,u}$ leads to the eigenvalue equation [23],

$$(\omega + u\bar{\lambda} - \Omega) Q_{\omega,u} = \mu \int du' dw' (u + u') g_{\omega'u'} Q_{\omega',u'}, \quad (5)$$

where $\bar{\lambda} \equiv \lambda + \varepsilon\mu$. The solution has to be of the form $Q_{\omega,u} = (A + Bu)/(\omega + u\bar{\lambda} - \Omega)$. Solutions exist if $\mu^{-1} = I_1 \pm \sqrt{I_0 I_2}$, where $I_n = \int d\omega du g_{\omega,u} u^n / (\omega + u\bar{\lambda} - \Omega)$. The system is stable if all Ω are purely real. A possible imaginary part, κ , is the exponential growth rate.

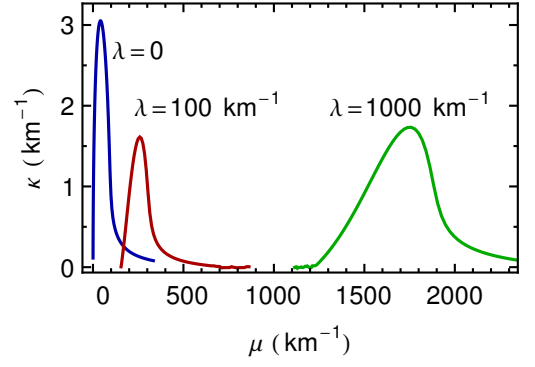


FIG. 3: Growth rate κ for our SN model as a function of μ for various λ values as indicated.

Application to our SN model.—Ignoring the effect of matter ($\lambda = 0$), we show $\kappa(\mu)$ for our 280 ms SN model in Fig. 3. The system is essentially stable above μ of a few 100 km^{-1} . It is noteworthy that κ is of the same order as a typical ω of the $g_{\omega,u}$ distribution, in our case a few km^{-1} . We also show $\kappa(\mu)$ for $\lambda = 10^2$ and 10^3 km^{-1} and observe a shift to larger μ -values [23].

In Fig. 4 we show contours of κ in the (μ, λ) plane. For large μ and λ values, the system is unstable for $\lambda \sim \mu$ [23]. In other words, if the local neutrino number density is much smaller or much larger than the local electron density, the system is stable.

We also show the locus of $[\mu(r), \lambda(r)]$ along the radial direction. Since $\mu(r) \propto r^{-4}$, the red solid line in Fig. 4 is essentially the SN density profile. The step-like feature is the shock wave where the matter density drops by an order of magnitude. Without matter ($\lambda = 0$), neutrinos would enter the instability strip at $\mu \sim 100$, correspond-

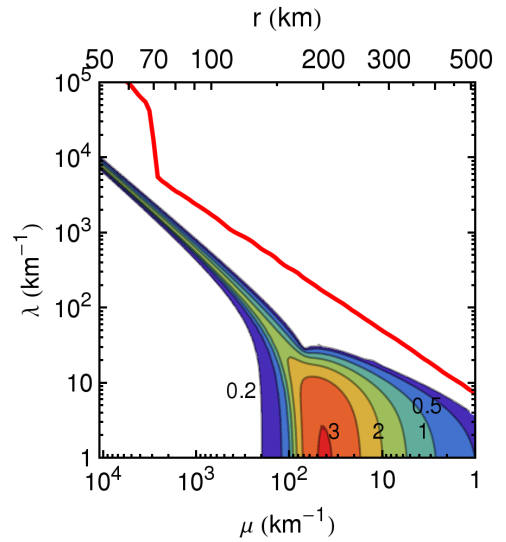


FIG. 4: Contours for the growth rate κ in km^{-1} . Also shown is the profile for our SN model. The vertical axis essentially denotes the density, the horizontal axis the radius ($\mu \propto r^{-4}$).

ing to $r \sim 150$ km. We find similar results for other snapshots at times 150 and 400 ms postbounce, i.e., neutrinos do not encounter a self-induced instability.

Comparison with earlier work.—A similar accretion-phase model of the Basel group was used to study flavor stability by numerically solving the EoMs [19]. A mono-energetic neutrino distribution and isotropic emission at a neutrino sphere were assumed. For some snapshots, an instability occurred at a large radius. Applying our method to the same matter profile and schematic neutrino distribution we find perfect agreement with Ref. [19] and even reproduce their onset radius for those cases where partial flavor conversion occurs [27]. It would be interesting to repeat our study with realistic Basel distributions to see if partial flavor conversion is an artifact of their schematic energy and angle distributions.

Conclusions.—We have performed a linearized flavor stability analysis of accretion-phase SN models and neutrino fluxes with realistic energy and angle distributions. For these models, self-induced flavor conversions do not occur. One should apply this method to a broader class of models to see if this conclusion is generic. It also remains to extend a linearized analysis to cases without cylindrical symmetry of the angular distribution in view of Sawyer’s concerns about a significant multi-angle instability [12]. In realistic 3D models, the neutrino distribution is not cylindrically symmetric and even if this were the case, in principle even a small fluctuation could trigger a novel instability if it were to exist.

Recent evidence suggests that the neutrino mixing angle θ_{13} is not very small [20], implying that the MSW conversion in the SN is adiabatic. One can then distinguish the neutrino mass hierarchy by Earth matter effects [3] or the early rise time [4], but only if collective oscillations do not swap flavors before the MSW region. (In the presence of the collective flavor swap, the hierarchy could be distinguished for an extremely small θ_{13} where the MSW conversion is not adiabatic [28].) The suppression of self-induced flavor conversion during the accretion phase, if generic, is good news for the possibility of determining the mass hierarchy with SN neutrinos if a “large” value for θ_{13} is experimentally confirmed.

We thank T. Hahn for helping to implement a numerical library [29]. We acknowledge partial support by DFG Grants No. TR 7, TR 27, EXC 153 and computer time at the HLRS in Stuttgart and NIC in Jülich.

[1] H.-T. Janka, K. Langanke, A. Marek, G. Martínez-Pinedo and B. Müller, Phys. Rept. **442**, 38 (2007).
 [2] D. Autiero *et al.*, JCAP **0711**, 011 (2007). M. Wurm *et al.*, arXiv:1104.5620. K. Scholberg, J. Phys. Conf. Ser. **203**, 012079 (2010).
 [3] A. S. Dighe and A. Yu. Smirnov, Phys. Rev. D **62**, 033007 (2000). A. S. Dighe, M. T. Keil and G. G. Raffelt, JCAP **0306** (2003) 005; JCAP **0306** (2003) 006.

[4] S. Chakraborty, T. Fischer, L. Hüdepohl, H.-T. Janka, A. Mirizzi and P. D. Serpico, arXiv:1111.4483.
 [5] L. Wolfenstein, Phys. Rev. D **17**, 2369 (1978).
 [6] S. P. Mikheev and A. Yu. Smirnov, Sov. J. Nucl. Phys. **42**, 913 (1985) [Yad. Fiz. **42**, 1441 (1985)]; Sov. Phys. JETP **64**, 4 (1986) [Zh. Eksp. Teor. Fiz. **91**, 7 (1986)].
 [7] T. K. Kuo and J. T. Pantaleone, Rev. Mod. Phys. **61**, 937 (1989).
 [8] J. Pantaleone, Phys. Lett. B **287**, 128 (1992).
 [9] G. Sigl and G. Raffelt, Nucl. Phys. B **406**, 423 (1993).
 [10] S. Samuel, Phys. Rev. D **48**, 1462 (1993); Phys. Rev. D **53**, 5382 (1996). V. A. Kostelecký and S. Samuel, Phys. Lett. B **318**, 127 (1993); Phys. Rev. D **52**, 621 (1995).
 [11] R. F. Sawyer, Phys. Rev. D **72**, 045003 (2005).
 [12] R. F. Sawyer, Phys. Rev. D **79**, 105003 (2009).
 [13] H. Duan, G. M. Fuller, J. Carlson and Y.-Z. Qian, Phys. Rev. D **74**, 105014 (2006).
 [14] B. Dasgupta, A. Dighe, G. Raffelt and A. Yu. Smirnov, Phys. Rev. Lett. **103**, 051105 (2009).
 [15] H. Duan, G. M. Fuller and Y.-Z. Qian, Annu. Rev. Nucl. Part. Sci. **60**, 569 (2010).
 [16] B. Dasgupta, E. P. O’Connor and C. D. Ott, arXiv:1106.1167. Y. Suwa, K. Kotake, T. Takiwaki, M. Liebendörfer and K. Sato, Astrophys. J. **738**, 165 (2011).
 [17] H. Duan, G. M. Fuller, J. Carlson and Y.-Z. Qian, Phys. Rev. Lett. **100**, 021101 (2008). B. Dasgupta, A. Dighe, A. Mirizzi and G. G. Raffelt, Phys. Rev. D **77**, 113007 (2008). J. F. Cherry, M. R. Wu, J. Carlson, H. Duan, G. M. Fuller and Y.-Z. Qian, Phys. Rev. D **84**, 105034 (2011).
 [18] A. Esteban-Pretel, A. Mirizzi, S. Pastor, R. Tomàs, G. G. Raffelt, P. D. Serpico and G. Sigl, Phys. Rev. D **78**, 085012 (2008).
 [19] S. Chakraborty, T. Fischer, A. Mirizzi, N. Saviano and R. Tomàs, Phys. Rev. D **84**, 025002 (2011); Phys. Rev. Lett. **107**, 151101 (2011).
 [20] K. Abe *et al.* (T2K Collaboration), Phys. Rev. Lett. **107**, 041801 (2011). G. L. Fogli, E. Lisi, A. Marrone, A. Palazzo and A. M. Rotunno, Phys. Rev. D **84** (2011) 053007. Y. Abe *et al.* (Double Chooz Collaboration), arXiv:1112.6353. P. A. N. Machado, H. Minakata, H. Nunokawa and R. Z. Funchal, arXiv:1111.3330.
 [21] H. Duan, G. M. Fuller and J. Carlson, Comput. Sci. Dis. **1**, 015007 (2008).
 [22] S. Hannestad, G. Raffelt, G. Sigl and Y. Y. Y. Wong, Phys. Rev. D **74**, 105010 (2006); Erratum *ibid.* **76**, 029901 (2007). H. Duan, G. M. Fuller, J. Carlson and Y. Z. Qian, Phys. Rev. D **75**, 125005 (2007). G. G. Raffelt, Phys. Rev. D **83**, 105022 (2011).
 [23] A. Banerjee, A. Dighe and G. Raffelt, Phys. Rev. D **84**, 053013 (2011).
 [24] L. Hüdepohl, B. Müller, H.-T. Janka, A. Marek and G. G. Raffelt, Phys. Rev. Lett. **104**, 251101 (2010); Erratum *ibid.* **105**, 249901 (2010).
 [25] S. E. Woosley, T. A. Weaver, Astrophys. J. Suppl. **101**, 181 (1995).
 [26] M. Rampp, H. T. Janka, Astron. Astrophys. **396**, 361 (2002).
 [27] S. Sarikas and G. Raffelt, arXiv:1110.5572.
 [28] B. Dasgupta, A. Dighe and A. Mirizzi, Phys. Rev. Lett. **101**, 171801 (2008).
 [29] T. Hahn, Comput. Phys. Commun. **168**, 78 (2005).